Design of a Novel P450: A Functional Bacterial−Human Cytochrome P450 Chimera†

Miyuki Shimoji,‡ Hequn Yin,§ LeeAnn Higgins,‡ and Jeffrey P. Jones*,‡

Departments of Biochemistry & Biophysics and Pharmacology & Physiology, University of Rochester, Rochester, New York 14642, and Department of Drug Metabolism and Pharmacokinetics, Hoffman-La Roche, Nutley, New Jersey 07110

Received November 11, 1997; Revised Manuscript Received January 14, 1998

ABSTRACT: We report the construction of a functional chimera from approximately 50% bacterial (cytosolic) cytochrome P450cam and 50% mammalian (membrane-bound) cytochrome P450 2C9. The chimeric protein shows a reduced CO-difference spectrum absorption at 446 nm, and circular dichroism spectra indicate that the protein is globular. The protein is soluble and catalyzes the oxidation of 4-chlorotoluene using molecular oxygen and reducing equivalents from bacterial putidaredoxin and putidaredoxin reductase. This chimera provides a novel method for addressing structure−function issues and may prove useful in the design of oxidants for benign and stereospecific synthesis, as well as catalysts for bioremediation of polluted areas. Furthermore, these results provide the first evidence that bacterial P450 enzymes and mammalian P450 enzymes are likely to share a common tertiary structure.

The cytochrome P450 enzyme family is responsible for the metabolism of a large number of drugs and environmental pollutants in mammals. If we could predict the rates and regioselectivities of metabolism of these xenobiotics, we could predict the half-life of most drugs and the potential for bioactivation of new drugs and assess the risk associated with environmental pollution (*1*). Furthermore, an increased understanding of the binding features and mechanistic details of this important class of enzymes can be used to design oxidants for benign and stereospecific synthesis, as well as catalysts for bioremediation of polluted areas (*2*).

To date, no three-dimensional structure of a mammalian P450 enzyme is available, despite the use of special expression vectors (*3*, *4*) and peptitergents to improve solubility (*5*). In contrast, the crystal structures of a number of cytosolic bacterial P450s have been determined. These include P450cam, P450BM3, P450terp, and P450eryF (*6*−*11*). Since no detailed structural information has been obtained for a mammalian P450 enzyme, all attempts to determine the effect of enzyme−substrate interactions have used the crystal structures from the soluble bacterial P450 enzymes (*12*). While homology models can be constructed for the membrane-bound mammalian enzymes on the basis of bacterial enzymes, the very low sequence identities (<20%) mean that any resulting model has low resolution (*13*). Despite these constraints, homology models can be constructed that successfully explain the results of site-directed mutagenesis experiments (*14*). However, no information to date directly supports the hypothesis that mammalian and bacterial enzymes are structurally related.

We chose to construct a chimera, P450BFG, that contained a portion of cytochrome P450 2C9 (see Figure 1) since this isoform of P450 is abundant in human liver and plays an important role in drug metabolism (*15*, *16*). We have already reported an active-site model of P450 2C9 based on ligand binding to this enzyme (*17*). Furthermore, the successful construction of a chimera from a bacterial and a mammalian source would help to validate the use of bacterial structures in constructing homology models of mammalian P450 enzymes.

EXPERIMENTAL PROCEDURES

Construction of an Expression Plasmid for P450BFG and Wild-Type P450cam. The homology model of P450BFG was produced with the program Modeler (*18*) and used the coordinates of P450cam, P450BM3, and P450eryF. We selected the position for fusion on the basis of the resulting homology model. The constuct of the expression plasmid is shown in Figure 2. Subcloning was performed in Epicurian Coli XL1-Blue MR supercompetent cells (Stratagene, La Jolla, CA). All modifications were introduced by PCR mutagenesis. Templates for PCR were pretreated with the alkaline-denaturing method (*19*), and then site-directed mutagenesis was performed with the ExSite PCR-Based Site-Directed Mutagenesis Kit (Stratagene). As shown in Figure 2, first, the *Nco*I restriction site was introduced in P450cam by primer 1 and 2 (amino acids 216−218) and P450 2C9 by primer 3 and 4 (amino acids 256−258). The starting position of the H-helix of P450 2C9 is aspartic acid 264. After digestion of *Xho*I (P450cam) or *Eco*RI (P450 2C9), each plasmid was blunt-ended and then digested by *Nco*I. The fragments of P450cam and P450 2C9 were ligated after the digestion by *Nco*I−*Xho*I or *Eco*RI. The ligated plasmid

† This work was supported in part by National Institutes of Health Grants GM32165 and ES05407 and National Science Foundation Grant BES-9710129.

* To whom correspondence should be addressed. Telephone: (716) 275-5371. Fax: (716) 244-9283. E-mail: jpj@cyp.medicine.rochester.edu.

‡ University of Rochester.

§ Hoffman-La Roche.

S0006-2960(97)02775-X CCC: $15.00
Published on Web 06/02/1998

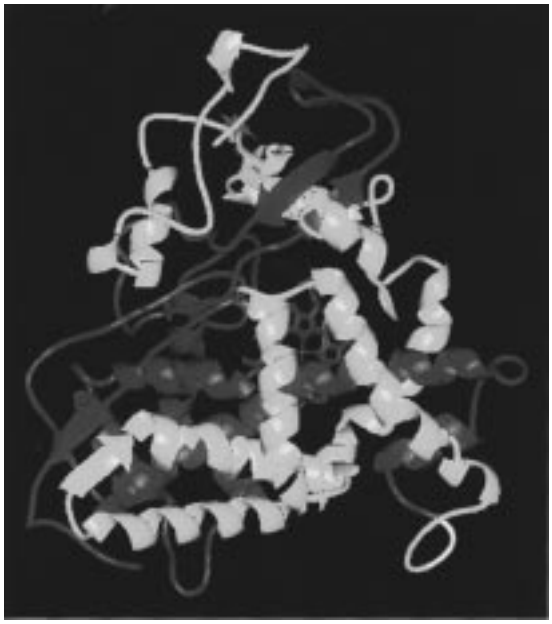

FIGURE 1: Model of the P450BFG structure. The yellow region is from P450cam, and the red region is from P450 2C9. The heme is shown in green. The white region is the site chosen for fusion of the bacterial and mammalian sequences.

contained P450cam, including the pBluescript vector, from the amino terminus to the G-helix (residues 1−216) and P450 2C9 from the H-helix to the carboxyl terminus (methionine 257 to the C terminus). In addition, the sequence at the junction (Ala-Met-Asp) was returned to the original sequence (Gly-Met-Asn) of P450cam and P450 2C9 by site-directed mutagenesis with primers 5 and 6. A $(His)_6$ affinity tag coding sequence was inserted at the 3′ terminus of P450 2C9 cDNA by primers 7 and 8. The sequences of primers are as follows: primer 1, CCATGGACGCTATCAGCATCGTTGCCAAC; primer 2, CCGGCTTCTGCCTGCGTTGCTCGA; primer 3, CCATGGACAACCCTCAGGACTTTATTGAT; primer 4, CCATTGATTCTTGGTGTTCTTTTACT; primer 5, GCATGAACAACCCTCAGGACTTTATTGA; primer 6, CCGGCTTCTGCCTGCGTTGCTCG; primer 7, CATCACCATCACCATCACTGAAGAAGAGCAGATGGCCTGGC; and primer 8, GACAGGAATGAAGCACAGCTGGTA. A $(His)_6$ affinity tag coding sequence was inserted at the 3′ terminus of P450cam cDNA.

Expression of the Fusion Protein. A single ampicillin-resistant colony of DH5α cells transformed with the plasmid DNA described above was cultured overnight at 37 °C in Luria-Bertani medium containing ampicillin (100 μg mL^{-1}). A 0.5 mL aliquot was used to inoculate 50 mL of Terrific broth (TB)[1] and the mixture cultured for 8 h at 37 °C. This 25 mL aliquot was used to inoculate 500 mL of TB at 30 °C. Incubation at 30 °C was continued for 48 h. The TB was supplemented with ampicillin (100 μg mL^{-1}), 0.5% glucose, 1 mM δ-aminolevulinic acid (δ-ALA, only for the 500 mL culture), vitamins (1% w/w, Basal Medium Eagle Vitamin Solution, Gibco BRL, Grand Island, NY), and trace elements [2 mM $MgSO_4 \cdot 7H_2O$, 0.1 mM $CaCl_2$, $FeSO_4$ (1.0 and 10.0 μM for the 50 and 500 mL cultures, respectively), and a metal solution (50 μM H_3BO_4, 0.2 μM $CoCl_2 \cdot 6H_2O$, 1 μM $CuSO_4 \cdot 5H_2O$, 1 μM $MnCl_2 \cdot 4H_2O$, 1 nM Na_2MoO_4, and 2 μM $ZnCl_2$)]. The cells were harvested by centrifugation at 5000*g* and 4 °C for 10 min. The pellet was stored at −80 °C before being used.

Expression of the Wild-Type P450cam. A methodology similar to that of the fusion protein was used except for the culture temperature and the concentration of δ-ALA. The small scale culture at 37 °C for 8 h was followed by the incubation at 37 °C for 21 h. The concentration of δ-ALA was 0.12 mM.

Purification and Analyses of the Expressed Chimeric and Wild-Type P450 Proteins. The suspension buffer for the bacterial pellet must contain 50 μM *d*-camphor. The supernatant was applied to a Ni-NTA agarose column (Qiagen Inc., Chatsworth, CA). The column was eluted with 10 column volumes of buffer A [50 mM sodium phosphate (pH 7.8) containing 300 mM NaCl, 50 μM *d*-camphor, 5 mM 2-mercaptoethanol, and 5% (v/v) glycerol] and eluted with buffer A containing 80 mM imidazole. The red-colored fractions were collected and dialyzed overnight at 4 °C against 2 L of buffer B [10 mM potassium phosphate (pH 7.2) containing 0.1 mM DTT, 0.1 mM EDTA, 50 mM *d*-camphor, and 5% (v/v) glycerol]. The sample was applied to a hydroxylapatite column (Bio-Rad Laboratories, Hercules, CA) equilibrated with buffer B and then eluted with a linear gradient of 10 to 300 mM potassium phosphate buffer (pH 7.2). The fractions with a strong red color were collected, and the protein purity (*20*) and P450 specific content were analyzed (*21*).

Circular Dichroism Experiments. Purified P450BFG and P450cam wild type were dialyzed for 3 h at 4 °C against 1 L of 52.6 mM potassium phosphate (pH 7.0) containing 263 mM KCl and 106 μM dithiothreitol. The dialyzed samples were used for circular dichroism experiments. Details of the experimental procedure are described elsewhere (*22*).

Construction, Expression, and Purification of Putidaredoxin (Pt) and Putidaredoxin Reductase (PtR). The *Nde*I restriction site was introduced at the site of the initiation codon of the Pt or PtR plasmids (*23*) by PCR mutagenesis. After digestion of Pt by *Sma*I and digestion of PtR by *Mlu*I followed by blunt ending, each plasmid was digested by *Nde*I, and gel-purified DNA was cloned into the pET-15 expression vector (Novagene, Madison, WI) after digestion by *Xho*I and blunt ending and digestion by *Nde*I. *Escherichia coli* strain BL21 (DE3) (Novagene) was transformed with pETPt or pETPtR. After Ni-NTA column chromatography, each expressed protein was further purified by DE 52 using the method described by Gunsalus and Wagner (*24*).

Assay of the Oxidation of 4-Chlorotoluene and Isotope Effect Measurements. Purified P450BFG, P450cam wild type, Pt, and PtR were each dialyzed for 3−6 h at 4 °C against 1 L of 50 mM potassium phosphate (pH 7.4) containing 200 mM KCl and 106 μM dithiothreitol before being used. The assays were carried out at 37 °C for 20 min in a 1 mL reaction mixture in 50 mM potassium phosphate (pH 7.4) containing 200 mM KCl. The reaction mixtures contained 0.5 mM 4-chlorotoluene and 1.5 μM wild-type P450cam or 0.1−0.4 μM P450BFG and 3 μM Pt, 1.5 μM PtR, and 0.3 mM NADH (*25*). P450 2C9 was obtained with the HepG2 vaccinia expression system de-

[1] Abbreviations: TB, Terrific broth; δ-ALA, δ-aminolevulinic acid; Pt, putidaredoxin; PtR, putidaredoxin reductase; SRS, substrate recognition site; CYP, cytochrome P450.

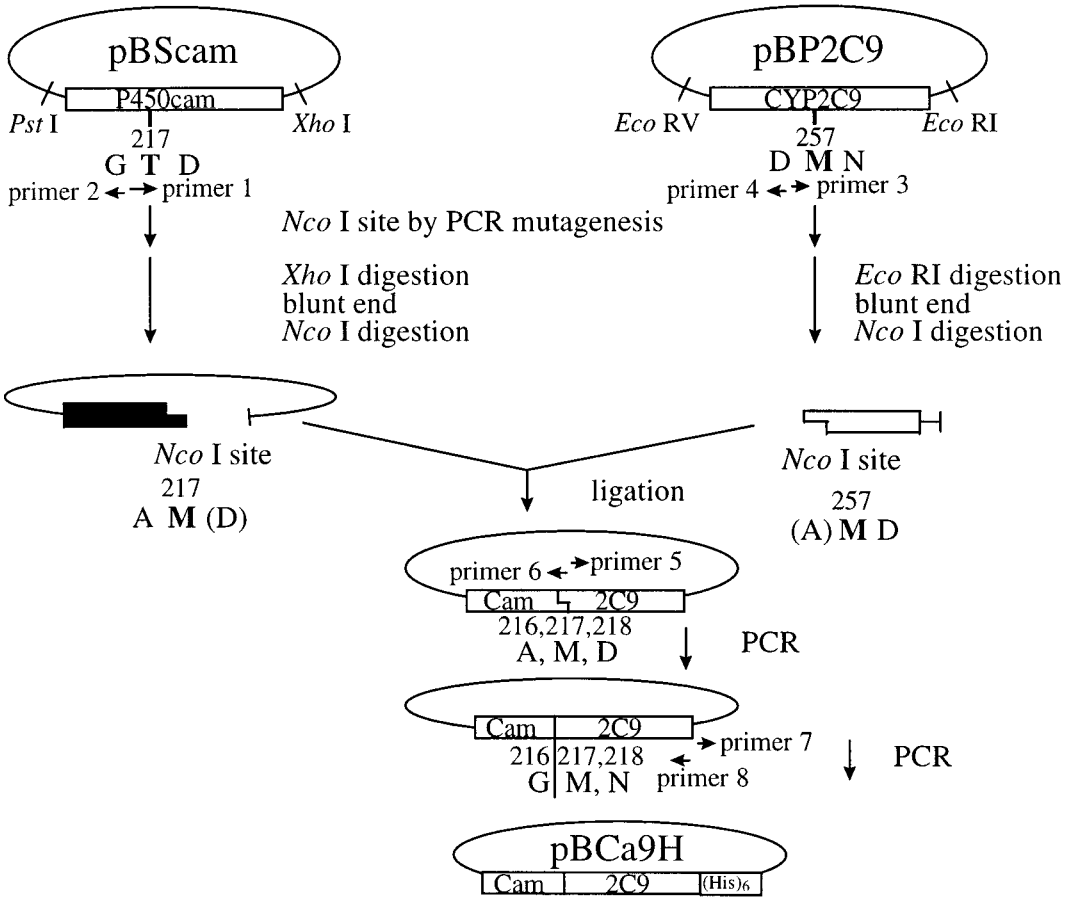

FIGURE 2: Construction of a fused plasmid of P450cam and P450 2C9.

scribed previously (*26*). The 4-chlorobenzyl alcohol metabolite was detected by gas chromatography−mass spectrometry (*27*). Details of the isotope effect measurements and experimental design were as described previously (*28*).

RESULTS AND DISCUSSION

Design and Construction of the P450cam−P450 2C9 Chimera. Our attempts to make a soluble chimeric construct were based on a homology model of P450 2C9 (*13*). The resulting homology model shown in Figure 1 suggested that replacing all amino acids prior to the random coil between the G- and H-helix [using the P450cam structural nomenclature (*7*)] with bacterial amino acids should provide a soluble bacterial−mammalian chimera. This coil was chosen on the basis of the hypothesis that the amino terminus and possibly the distal face of the protein (comprised of amino acids prior to the coil) were involved in membrane interactions. Since the sequence alignments are based on very low sequence identity, we chose an area for fusion with no secondary structure to increase our chances of producing a folded protein.

A single chimera was constructed to have the P450cam primary sequence from the amino terminus to the G-helix (residues 1−216) and the P450 2C9 primary sequence from before the putative H-helix to the carboxyl terminus (methionine 257 to the C terminus) (Figures 1 and 2). According to the nomenclature of Gotoh (*29*), the active site would be composed of SRS (substrate recognition site) 1−3 from P450cam and SRS 4−6 from P450 2C9. A $(His)_6$ affinity tag coding sequence was inserted at the 3′ terminus of the P450 2C9 cDNA to allow protein purification by affinity chromatography (*30*, *31*). The chimera was expressed in *E. coli* with the pBluescript vector.

Expression of P450 Proteins and Solubility. A typical preparation of chimera yielded around 200 nmol/L, while the expression levels of the wild-type P450cam were 600−1000 nmol/L under similar conditions. After treatment with lysozyme and sonication of the cell pellet, the cell lysate was centrifuged at 105000*g* and the supernatant was found to contain all the P450. This protein was purified with a Ni-NTA agarose column followed by a hydroxylapatite column. The fact that the resulting enzyme is soluble, while mammalian enzymes with the amino terminus removed are not, indicates that other regions near the amino terminus may also be important for membrane interactions (*32*−*35*).

Identification and Spectra Studies. The purified P450BFG showed one major and one minor band on SDS−polyacrylamide gel electrophoresis (Figure 3). The major band showed an approximate molecular mass of 51 kDa as judged by SDS−polyacrylamide gel electrophoresis, consistent with the molecular mass expected from the component segments (Figure 3). Similarly, two bands are observed for wild-type P450cam prepared with a $(His)_6$ tag coding sequence. The minor lower-molecular mass band is at present unidentified. In the presence of imidazole, the absolute spectrum of the wild-type P450cam showed a maximum peak at 417 nm, which indicates that the heme is predominantly in the low-

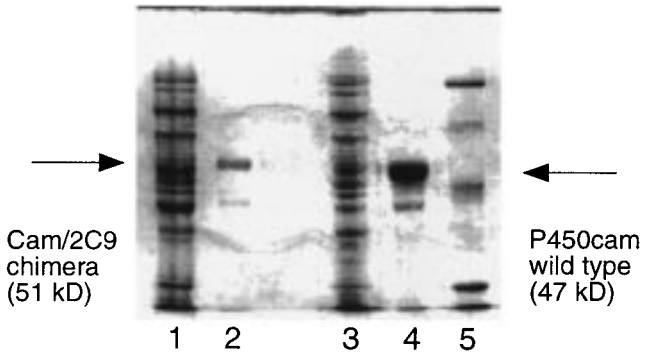

FIGURE 3: SDS−polyacrylamide gel electrophoresis of P450BFG expressed in *E. coli*. Lanes 1 and 2 show the fusion protein, and lanes 3 and 4 show wild-type P450cam: lane 1, 105000*g*-centrifuged supernatant (3 μg of protein); lane 2, eluate from a hydroxylapatite column (1.5 μg of protein); lane 3, 105000*g*-centrifuged supernatant (3 μg of protein); lane 4, eluate from a hydroxylapatite column (2.2 μg of protein); and lane 5, molecular mass markers. The gel was stained with Coomassie Brilliant Blue R250.

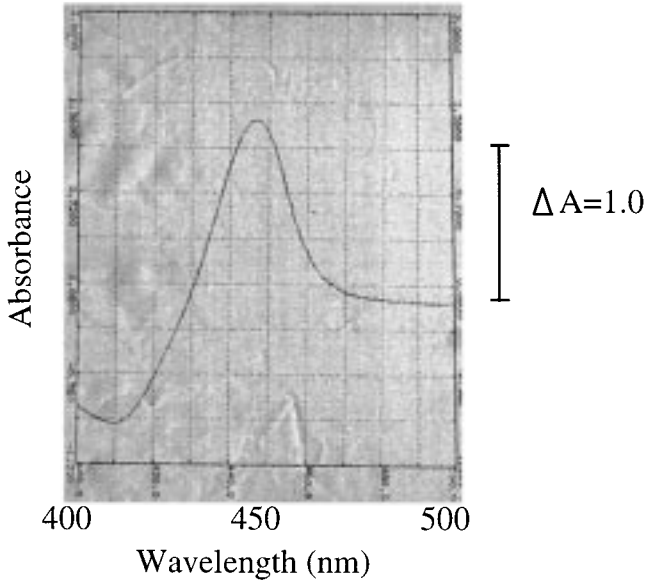

FIGURE 4: CO-reduced difference spectrum of P450BFG with an absorbance maximum at 446 nm. The preparation used corresponds to that from lane 2 in Figure 3.

spin state. The spin state of the chimera was mainly high-spin in the presence of imidazole, with a maximum absorbance at 393 nm (data not shown).

The purified P450BFG showed a reduced CO-difference spectrum at 446 nm (Figure 4) characteristic of a functional P450 protein. The specific content of P450BFG was 6.4 nmol/mg of protein. For P450 enzymes, the presence of a CO-difference spectrum is taken as evidence that the protein is folded and has incorporated heme. However, since a CO-difference spectrum is only an indirect measure of whether the chimeric protein has folded, we performed circular dichroism studies to explore the secondary structure of P450BFG. The spectrum of the chimera showed a typical helical structure (data not shown), and the secondary structure predicted on the basis of these studies is presented in Table 1. Thus, the circular dichroism studies confirm that the chimera is folded. While the secondary structural features are similar to those expected for a P450 protein, they are not identical to those of P450cam.

Table 1: Comparison of the Structural Properties and Activities of the Fusion Protein with Bacterial P450cam and Expressed Human P450 2C9

	α-helix (%)[a]	β-sheet (%)[a]	product formation	KIE[b]
P450BFG	35.5	5.4	0.167[c]	5.8
P450cam	28.8	18.0	0.078[c]	6.5
P450 2C9	nd[d]	nd[d]	0.158[e]	6.2

[a] The results from circular dichroism experiments. Repeated experiments showed similar results. [b] Intramolecular kinetic isotope effect for 4-chlorotoluene-α-$^2H_2$. [c] Nanomoles of 4-chlorobenzyl alcohol per minute per nanomole of P450. [d] Value not determined. [e] Nanomoles per minute milligram of protein from microsomal fractions of expressed CYP 2C9. Each of the values for product formation and isotope effects is the mean of two or three separate experiments performed on different days.

The fact that the two proteins can be fused and fold to give a functional protein provides evidence that the bacterial P450cam and the mammalian P450 2C9 may share common tertiary structure. However, an alternate explanation is that the bacterial and mammalian enzymes do not share a common tertiary structure but, when combined to form a chimera, can fold to form a functional protein with a novel structure. This explanation could certainly be possible if the proteins were constructed from multiple domains and we were fusing these different domains. However, this seems unlikely, as neither the crystal structures of P450cam nor those of other bacterial proteins show any evidence that multiple domains exist. In each case, the entire sequence surrounds the heme, and residues from near the beginning of the amino terminus to near the end of the carboxyl terminus are important in heme binding or substrate binding.

Catalytic Activity and Electronic Features of the Active Oxygen. Next, the ability of the fusion protein to oxidize a P450 substrate was determined. The bacterial and mammalian enzymes both require an electron-transfer protein(s) to reduce molecular oxygen prior to formation of an active monooxygen species (*23*, *36*). However, the bacterial and mammalian enzymes use different, unrelated electron-transfer systems. For these experiments, we purified Pt and PtR after subcloning each cDNA into a pET vector with the *T7lac* promoter and a $(His)_6$ tag coding sequence. We found that this bacterial electron-transfer system could support the oxidation of 4-chlorotoluene to 4-chlorobenzyl alcohol by P450BFG. Thus, the fusion protein can function as an active P450 enzyme (Table 1). In fact, P450BFG showed slightly higher activity toward this substrate than P450cam. Experiments to determine if the mammalian P450 reductase can support the same oxidation with P450BFG are underway.

To examine if the electronic nature of the active oxygen is perturbed in P450BFG, we determined the magnitude of the intramolecular deuterium kinetic isotope effect for the hydroxylation of 4-chlorotoluene and compared it with the isotope effects for the same reaction catalyzed by P450cam and P450 2C9. The resulting isotope effects (Table 1) are essentially the same for each enzyme, indicating that the reactivity of the active oxygen is likely to be the same for each enzyme. While the isotope effects indicate that the active oxygen reactivities are the same, it is possible that this agreement is fortuitous. To confirm that the proteins have the same reactivities, we will determine the isotope

effect profiles for each enzyme (*37*). This work is currently underway.

Potential Application of the Chimeric Construct. This approach to the construction of chimeras could have a number of applications. (1) From other homology models of mammalian P450 enzymes, it is apparent that this method may prove to be an interesting method for constructing soluble P450 enzymes with mammalian active-site characteristics. These enzymes should be more adaptable to uses in bioremediation than the more restrictive bacterial enzymes and easier to work with than the membrane-bound mammalian enzymes. (2) Since the enzyme is soluble, it could provide a method for obtaining structural information. In particular, it should be amenable to X-ray crystallography. (3) If structural information can be obtained, chimeric enzymes could play an important role in the design of enzymes for selective oxidation reactions in the synthesis of organic compounds. (4) Selectively replacing amino acid segments in the amino terminus with the mammalian amino acids may prove to be a valuable method for determining important membrane association sites. (5) Since the enzyme is part mammalian and part bacterial, it can be used to determine the features that confer specific interactions with the different reductase systems.

In conclusion, the observation that a chimera of P450 2C9 and P450cam, which have less than 15% primary sequence identity, can still fold provides evidence for a conserved three-dimensional structure between P450cam and the CYP2 family.

ACKNOWLEDGMENT

We thank Dr. Thomas Poulos for suggesting the CD experiment, Andre Sali for Modeler, J. Peterson for P450cam, putidaredoxin, and putidaredoxin reductase cDNA, and F. Gonzalez for P450 2C9 cDNA. We are thankful for the advice and comments from Drs. B. Goldstein and T. Kamataki.

REFERENCES

1. Jones, J. P., and Korzekwa, K. R. (1996) *Methods Enzymol. 272*, 326−335.
2. Poulos, T. L. (1991) *Methods Enzymol. 206*, 11−30.
3. Sandhu, P., Baba, T., and Guengerich, F. P. (1993) *Arch. Biochem. Biophys. 306*, 443−450.
4. Haining, R. L., Hunter, A. P., Veronese, M. E., Trager, W. F., and Rettie, A. E. (1996) *Arch. Biochem. Biophys. 333*, 447−458.
5. Sueyoshi, T., Park, L. J., Moore, R., Juvonen, R. O., and Negishi, M. (1995) *Arch. Biochem. Biophys. 322*, 265−271.
6. Poulos, T. L., Finzel, B. C., Gunsalus, I. C., Wagner, G. C., and Kraut, J. (1985) *J. Biol. Chem. 260*, 16122−16130.
7. Poulos, T. L., Finzel, B. C., and Howard, A. J. (1987) *J. Mol. Biol. 195*, 685−700.
8. Ravichandran, K. G., Boddupalli, S. S., Hasemann, C. A., Peterson, J. A., and Deisenhofer, J. (1993) *Science 261*, 731−736.
9. Hasemann, C. A., Ravichandran, K. G., Peterson, J. A., and Deisenhofer, J. (1994) *J. Mol. Biol. 236*, 1169−1185.
10. Hasemann, C. A., Kurumbail, R. G., Boddupail, S. S., Peterson, J. A., and Deisenhofer, J. (1995) *Structure 3*, 41−62.
11. Cupp-Vickery, J. R., Li, H., and Poulos, T. L. (1994) *Proteins 20*, 197−201.
12. Paulsen, M. D., Manchester, J., and Ornstein, R. L. (1996) *Methods Enzymol. 272*, 337−346.
13. Korzekwa, K. R., and Jones, J. P. (1993) *Pharmacogenetics 3*, 1−8.
14. He, Y. A., He, Y. Q., Szklaz, G. D., and Halpert, J. R. (1997) *Biochemistry 36*, 8831−8839.
15. Goldstein, J. A., and Morais, S. M. F. (1994) *Pharmacogenetics 4*, 285−299.
16. Sullivan-Klose, T. H., Ghanayem, B. I., Bell, D. A., Zhang, Z. Y., Kaminsky, L. S., Shenfield, G. M., Miners, J. O., Birkett, D. J., and Goldstein, J. A. (1996) *Pharmacogenetics 6*, 341−349.
17. Jones, J. P., He, M., Trager, W. F., and Rettie, A. E. (1996) *Drug Metab. Dispos. 24*, 1−6.
18. Sali, A., and Blundell, T. L. (1993) *J. Mol. Biol. 234*, 779−815.
19. Dorrell, N., Gyselman, V. S., Foynes, S., Li, S. R., and Wren, B. W. (1996) *BioTechniques 21*, 604−608.
20. Laemmli, U. K. (1970) *Nature 227*, 680−685.
21. Omura, T., and Sato, R. (1964) *J. Biol. Chem. 239*, 2370−2378.
22. Pfeil, W., Nolting, B. O., and Jung C. (1993) *Biochemistry 32*, 8856−8862.
23. Peterson, J. C., Lorence, M. C., and Amarneh, B. (1990) *J. Biol. Chem. 265*, 6066−6073.
24. Gunsalus, I. C., and Wagner, G. C. (1978) *Methods Enzymol. 52*, 166−187.
25. Li, S., and Wackett, L. P. (1993) *Biochemistry 32*, 9355−9361.
26. White, R. E., and McCarthy, M.-B. (1986) *Arch. Biochem. Biophys. 246*, 19−32.
27. Gonzalez, F. J., Aoyama, T., and Gelboin, H. V. (1991) *Methods Enzymol. 206*, 85−92.
28. Iyer, K. R., Jones, J. P., Darbyshire, J. F., and Trager, W. F. (1997) *Biochemistry 36*, 7136−7143.
29. Gotoh, O. (1992) *J. Biol. Chem. 267*, 83−90.
30. Imai, T., Globerman, H., Gertner, J. M., Kagawa, N., and Waterman, M. R. (1993) *Proc. Natl. Acad. Sci. U.S.A. 268*, 19681−19689.
31. Kempf, A. C., Zanger, U. M., and Meyer, U. A. (1995) *Arch. Biochem. Biophys. 321*, 277−288.
32. Lemos-Chiarandine, C. D., Frey, A. B., Sabatini, D. D., and Kreibich, G. (1987) *J. Cell Biol. 104*, 209−219.
33. Vergeres, G., Winterhalter, K. H., and Richter, C. (1989) *Biochemistry 28*, 3650−3655.
34. Wachenfeldt, C., Richardson, T. H., Cosme, J., and Johnson, E. F. (1997) *Arch. Biochem. Biophys. 339*, 107−114.
35. Pernecky, S. J., and Coon, M. J. (1996) *Methods Enzymol. 272*, 25−34.
36. Estabrook, R. W., Shet, M. S., Ficher, C. W., Jenkins, C. M., and Waterman, M. R. (1993) *Arch. Biochem. Biophys. 333*, 308−315.
37. Manchester, J. I., Dinnocenzo, J. P., Higgins, L., and Jones, J. P. (1997*) J. Am. Chem. Soc. 119*, 5069−5070.

BI972775Z